Applied Science, Computing and Energy, 2026, 4(6), 863-881

Geology And Geochemistry of Rare Earth Element (REE)-Bearing Pegmatites Around Gwon-Gwon, Wamba Area, North-Central Nigeria

Manalaku Yele Pes, Nathaniel Goter Gokiand and Benson Shedrach Jatau

Received: 16 April 2026/Accepted: 20 August 2026/ Published: 24 August 2026

Abstract: *Rare earth element (REE)-bearing pegmatites are important exploration targets because they can concentrate critical metals during the final stages of granitic differentiation. This study evaluates the geology, structural controls, and whole-rock geochemistry of pegmatites around Gwon-Gwon, Wamba, North-Central Nigeria. Detailed mapping, structural measurements, and geochemical analyses were undertaken on eighteen representative pegmatite samples. The pegmatites occur mainly as discordant veins, ridge-forming bodies, and lenticular intrusions within migmatitic gneisses and leucogranites, with dominant NE–SW, ENE–WSW, N–S and subordinate NW–SE structural trends. Major-element data show decreasing MgO, Fe_2O_3, CaO, TiO_2 and P_2O_5 with increasing SiO_2, indicating progressive fractional crystallization. A/CNK–A/NK relations indicate predominantly metaluminous to weakly peraluminous compositions. Trace-element data show enrichment in Rb, Cs, Nb, Ta, Sn and selected REEs, while decreasing K/Rb ratios with increasing Rb indicate advanced magmatic differentiation. Tectonomagmatic discrimination places most samples in a late- to post-orogenic setting related to Pan-African granitic magmatism. The integrated evidence indicates that the pegmatites represent evolved residual melts emplaced along pre-existing structural discontinuities and possess significant rare-metal fertility, warranting further mineralogical and exploration investigation.*

Keywords: *Rare-earth elements; pegmatite; Pan-African Basement Complex; whole-rock geochemistry; fractional crystallization; rare-metal mineralization; Wamba; Nigeria.*

Manalaku Yele Pes
Solid Minerals Development Fund, Nigeria
Email: yelepes92@gmail.com
https://orcid.org/0009-0006-1655-806X

Nathaniel Goter Goki
Department of Geology and Mining, Nasarawa State University, Keffi, Nigeria
Email: Nathgoki@nsuk.edu.ng

Benson Shedrach Jatau
Department of Geology and Mining, Nasarawa State University, Keffi, Nigeria
Email: bsjatau@yahoo.co.uk

1.0 Introduction

Rare earth elements (REEs), together with Y and Sc, are important critical raw materials for high-technology, energy, electronics and defence applications. Growing demand has increased interest in geological environments capable of concentrating these elements. Granitic pegmatites are particularly significant because they commonly represent highly evolved products of granitic magmatism in which incompatible elements and volatile components become concentrated in residual melts. (Černý, 1991; Obaje, 2009).

The economic significance of REE-bearing pegmatites is related not only to the abundance of individual rare earth elements but also to their association with other critical and rare metals, including Nb, Ta, Sn, Y, Zr, Li, Cs and Be. Consequently, understanding the processes responsible for the concentration and redistribution of these elements is essential for evaluating pegmatite fertility and developing effective mineral exploration strategies.

Pegmatite evolution is controlled mainly by fractional crystallization, volatile enrichment, fluid–melt interaction and emplacement structures. Progressive crystallization removes major rock-forming minerals and concentrates incompatible elements such as Li, Rb, Cs, Be, Nb, Ta, Sn, U, Th and REEs. K/Rb, Rb/Sr, Cs/Rb, Nb/Ta, Ta/Sn, alumina saturation indices and normalized REE patterns are therefore useful indicators of magmatic evolution and rare-metal fertility. (Černý, 1991; El-Bouseily & El-Sokkary, 1975), During progressive magmatic differentiation, systematic variations in major and trace elements provide important evidence for the evolution of pegmatitic melts. Ratios such as K/Rb, Rb/Sr, Nb/Ta and Ta/Sn, together with REE patterns and alumina saturation indices, can therefore be used to distinguish relatively primitive pegmatitic melts from highly evolved and potentially mineralized systems. Integration of these geochemical indicators with field relationships and structural data provides a more reliable basis for interpreting pegmatite petrogenesis and mineralization potential.

Rare-metal pegmatites are commonly grouped into LCT and NYF families. LCT systems are generally associated with highly fractionated peraluminous granites and enrichment in Li, Cs, Ta, Sn, Be and Rb, whereas NYF systems are more commonly associated with metaluminous to weakly peraluminous A- or I-type granites and enrichment in Nb, Y, Zr, HREEs, U, Th and F. Transitional characteristics may occur, so classification should integrate field, mineralogical and geochemical evidence. (Černý & Ercit, 2005; Chappell & White, 1974). Although the LCT and NYF classifications provide a useful framework for interpreting rare-metal pegmatites, natural pegmatite systems may display overlapping or transitional geochemical characteristics. Their classification and genetic interpretation therefore require integration of whole-rock chemistry with host-rock relationships, structural setting, mineral assemblages and regional tectonomagmatic history.

The aim of this study is to investigate the geology, structural controls and whole-rock geochemistry of the REE-bearing pegmatites around Gwon-Gwon, Wamba, with a view to understanding their magmatic evolution, elemental enrichment, tectonomagmatic affinity and rare-metal fertility. Specifically, the study seeks to characterize their lithological relationships and field occurrence, determine the structural controls on emplacement, evaluate major-, trace- and REE-element distributions, assess the degree of magmatic differentiation, and establish their implications for rare-metal exploration.The Gwon-Gwon pegmatite field occurs within Wamba Local Government Area of Nasarawa State and is underlain mainly by migmatitic gneisses, leucogranites and pegmatites. Field relationships indicate that pegmatites cross-cut the older basement and granitoids and are associated with fractures and shear zones. Despite the recognized prospectivity of the Wamba district, the Gwon-Gwon pegmatites remain insufficiently characterized in terms of their lithological relationships, structural controls, degree of magmatic differentiation, trace-element and REE enrichment, and tectonomagmatic affinity. In particular, there is limited integrated information linking their field occurrence and structural architecture with whole-rock geochemical indicators of pegmatite evolution and rare-metal fertility. This knowledge gap limits a robust understanding of the petrogenesis and exploration significance of the Gwon-Gwon pegmatites. Addressing these uncertainties requires an integrated approach that combines geological mapping, structural analysis and whole-rock geochemistry. Such an approach can establish the relationship between the pegmatites and their host rocks, identify the principal structural pathways of emplacement, evaluate the extent of magmatic differentiation, and determine the distribution and behaviour of economically significant incompatible elements and REEs.The Nigerian Basement Complex forms part of the Trans-Saharan Mobile Belt and comprises migmatitic and gneissic complexes, schist belts, Pan-African granitoids, and abundant pegmatite intrusions. Numerous rare-metal pegmatite districts occur across north-central and northwestern Nigeria, including the Wamba, Nasarawa, Keffi, Egbe, Komu, Lema, and Kazaure pegmatite fields, many of which have attracted increasing exploration interest because of their lithium and REE potential. Previous investigations have demonstrated that many Nigerian pegmatites exhibit advanced magmatic differentiation, elevated concentrations of incompatible elements, and significant economic potential. However, the degree of fractionation, elemental enrichment and mineralization style varies considerably among individual pegmatite fields. Differences in parental magma composition, depth of emplacement, structural architecture, degree of fractionation and post-magmatic alteration may influence the distribution and concentration of rare metals and REEs. Consequently, regional generalizations cannot adequately explain the geological and geochemical characteristics of individual pegmatite occurrences.(Dada, 2006; Ekwueme & Matheis, 1995; Obaje, 2009; Oyawoye, 1972; Rahaman, 1988).

In Nigeria, rare-metal pegmatites are widespread within the Precambrian Basement Complex and are commonly associated with late Pan-African granitic magmatism. Previous studies have documented variations in their mineralogy, structural setting and geochemical signatures across different pegmatite provinces, demonstrating that their metallogenic characteristics are not uniform. Such variations emphasize the need for detailed investigations at individual pegmatite fields to establish their specific petrogenetic evolution and mineralization potential.

The Gwon-Gwon pegmatite field, situated within Wamba Local Government Area of Nasarawa State, lies within one of the most prospective pegmatite provinces of the Nigerian Basement Complex. The area is underlain predominantly by migmatitic gneisses, leucogranites, and pegmatite intrusions emplaced during the Pan-African orogeny. Field evidence indicates that the pegmatites occur as discordant veins, lenses, and ridge-forming bodies that intrude both granitoids and metamorphic basement rocks. Their close association with regional fracture systems and shear zones suggests that structural architecture exerted a fundamental control on magma emplacement and subsequent fluid migration. In addition, artisanal mining activities within and around the study area indicate the presence of economically significant rare-metal mineralization, highlighting the need for detailed scientific investigation. (Abaa, 1983; Dada, 2006; Obaje, 2009).

The significance of this study lies in providing an integrated geological and geochemical framework for understanding the Gwon-Gwon pegmatite system and its potential for rare-metal mineralization. The findings will contribute to knowledge of Pan-African pegmatite magmatism in the Nigerian Basement Complex, improve understanding of the structural and geochemical processes controlling REE and incompatible-element enrichment, and provide baseline information for future mineralogical, geochemical and exploration studies in the Wamba region. The results may also assist in identifying prospective zones for detailed exploration and support the broader assessment of Nigeria's critical-mineral resources.

2. 0 *Geological Setting*

2.1 Regional Geological Framework

The study area lies within the Precambrian Basement Complex of north-central Nigeria, part of the Trans-Saharan Mobile Belt. The regional geological framework is particularly important for interpreting the Gwon-Gwon pegmatites because the Pan-African tectonothermal event provided the structural and magmatic conditions necessary for the generation and emplacement of late granitic and pegmatitic melts. The interaction between inherited basement structures and late-stage magmatism may therefore have played a significant role in controlling the distribution and orientation of pegmatite bodies in the region.The regional basement comprises migmatitic–gneissic complexes, schist belts, Pan-African granitoids and late pegmatite and quartz-vein intrusions. Earlier crustal components were reworked during successive tectonothermal events culminating in the Pan-African Orogeny, which produced regional metamorphism, granitoid emplacement, ductile deformation and extensive pegmatite intrusion. (Abaa, 1983; Dada, 2006; Obaje, 2009; Oyawoye, 1972; Rahaman, 1988)

During Pan-African evolution, crustal thickening, partial melting and granitic magmatism generated residual melts enriched in incompatible elements. These melts migrated through fractures, shear zones and other crustal discontinuities during late- to post-collisional deformation. This relationship provides the regional framework for interpreting the structural emplacement and geochemical evolution of the Gwon-Gwon pegmatites. (Abaa, 1983; Dada, 2006).

2.2 Geology of the Wamba Pegmatite Field

The Wamba district is one of the important rare-metal pegmatite provinces of north-central Nigeria. Pegmatites occur as veins, lenses and irregular dykes associated spatially with Pan-African granitoids and older basement rocks. Reported mineral assemblages include quartz, feldspar, muscovite, tourmaline, beryl, garnet, cassiterite and Nb–Ta-bearing phases, with locally elevated concentrations of incompatible lithophile elements. Their close association with granitic bodies and regional structures supports emplacement from evolved residual melts. (Ekwueme & Matheis, 1995; Obaje, 2009).

he diversity of mineral assemblages and incompatible-element enrichment reported from the Wamba pegmatite district suggests variable degrees of magmatic evolution among individual pegmatite bodies. However, the extent to which these variations reflect differences in parental magma composition, fractional crystallization, structural emplacement or late-stage hydrothermal modification requires evaluation at the individual occurrence scale.

2.3 Local Geology of the Gwon-Gwon Area

The Gwon-Gwon area is underlain predominantly by migmatitic gneisses, leucogranites and pegmatites. Migmatitic gneiss forms the principal country rock and is medium- to coarse-grained, strongly foliated and composed mainly of quartz, feldspar and biotite. Leucogranites are coarse-grained and leucocratic, consisting mainly of quartz, K-feldspar, plagioclase and biotite, and field relationships show that they intrude the basement and are subsequently cut by pegmatites.

Pegmatites are the youngest and most conspicuous intrusive unit. Eighteen occurrences were mapped; individual bodies range from about 0.6 to 3 m in thickness, while the longest exposed veins exceed 200 m along strike. They are predominantly discordant, ridge-forming or lenticular and consist mainly of quartz, K-feldspar, plagioclase and mica, with accessory tourmaline and other rare-metal phases. Several bodies contain quartz-rich cores and evidence of late-stage alteration. Weathered exposures commonly show feldspar kaolinization, iron-oxide staining and lateritic development. These field relationships provide direct evidence for the intrusive nature of the pegmatites and their close spatial association with the host-rock structural fabric. However, the genetic significance of these relationships is evaluated in conjunction with the structural and geochemical results presented in subsequent sections.

2.4 Structural Framework

The structural framework is dominated by fractures, joints, foliation, shear zones and pegmatite-filled veins. Measurements indicate NE–SW, ENE–WSW and N–S as the principal trends, with subordinate NW–SE orientations. Pegmatites are generally steeply dipping (80–90°) and occupy pre-existing fractures and shear zones. Rose-diagram analysis shows close correspondence between pegmatite orientations and fracture sets, indicating that structural discontinuities provided important pathways for magma emplacement. Local brittle reactivation and fracture intersections may also have enhanced permeability for late-stage fluids.

The preferential alignment of pegmatite bodies along these structural trends suggests that pre-existing discontinuities provided zones of reduced mechanical resistance and enhanced permeability for the migration and emplacement of late-stage felsic melts. The intersections of differently oriented structures may also have created favourable sites for melt accumulation and subsequent fluid-assisted mineralization.

2.5 Geological Significance

The field relationships indicate a sequence of basement metamorphism, Pan-African granitoid emplacement, magmatic differentiation and late pegmatite intrusion. The association of pegmatites with leucogranites and structural discontinuities supports a model in which volatile-rich residual melts migrated through pre-existing crustal structures during the waning stages of Pan-African magmatism. The observed incompatible-element enrichment further supports the rare-metal prospectivity of the field. (Abaa, 1983; Dada, 2006).

3.0 Materials and Methods

3.1 Study Design

An integrated field and laboratory approach was used to establish lithological relationships, structural controls and geochemical evolution of the Gwon-Gwon pegmatites.

3.2 Desk Study and Pre-Field Preparation

Published geological literature, regional maps, topographic sheets, satellite imagery and previous research were reviewed before fieldwork. Sheet 189

SE (Kurra), at 1:25,000 scale, together with satellite imagery, was used to plan traverses, identify lineaments and optimize field coverage.

3.3 Geological Mapping

Detailed geological mapping covered approximately 36 km² during two field campaigns. Traverses followed footpaths, streams, artisanal workings, road cuts and natural exposures. Observations focused on lithology, contacts, weathering, mineralogy, texture, fabric, pegmatite morphology, structural relationships and evidence of alteration or mineralization. Outcrop locations and geological boundaries were recorded by handheld GPS and field observations were compiled into the geological map.

3.4 Sample Collection

Representative fresh samples were collected from pegmatites and associated host rocks to minimize weathering effects. Each sample was georeferenced, assigned a unique code and described in terms of lithology, mineral assemblage, structural setting and weathering. Eighteen representative pegmatite samples were selected for laboratory analysis based on spatial distribution and lithological variability.

3.5 Structural Analysis

Structural measurements were obtained with a Brunton compass from pegmatite veins, fractures, joints, foliation, shear zones, faults and quartz veins. Measurements from representative outcrops were used to characterize the structural framework and evaluate controls on pegmatite emplacement. Circular statistical analysis was used to generate rose diagrams and identify dominant orientations.

3.6 Sample Preparation

Samples were cleaned, oven-dried, crushed in a steel jaw crusher and pulverized in an agate mill to <75 µm. Equipment was cleaned between samples to minimize cross-contamination, and representative powders were retained for major-, trace- and REE analysis.

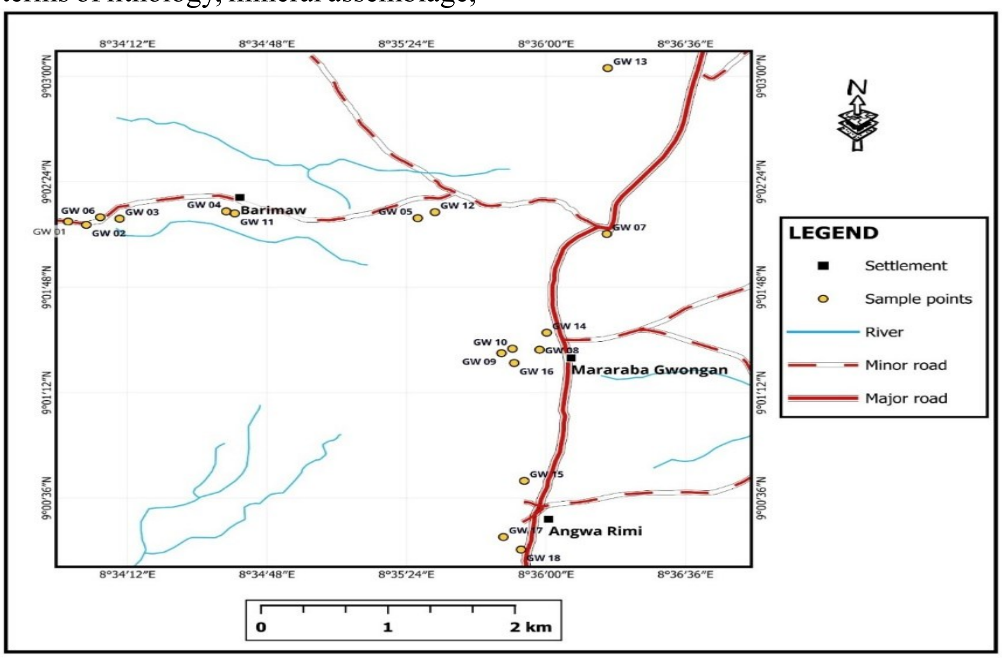

Fig. 1: Sample Point Map

3.7 Geochemical Analysis

Whole-rock major oxides were determined by X-ray Fluorescence Spectrometry (XRF), while trace-element and REE concentrations were determined using appropriate geochemical analytical techniques. Major-element data were evaluated with Harker, A/CNK–A/NK, SiO_2–K_2O and R_1–R_2 diagrams, while K/Rb relationships were used to assess fractionation. Trace-element and REE data were examined using chondrite-normalized REE patterns, primitive mantle-normalized spider diagrams, Rb–Sr and K/Rb–Cs relationships, and selected incompatible-element ratios. (El-Bouseily & El-Sokkary, 1975).

3.8 Data Processing and Interpretation

Geochemical data were subjected to descriptive evaluation and standard geochemical plotting. Structural measurements were treated using circular statistics. Interpretation followed established discrimination schemes including Shand (1943), Irvine and Baragar (1971), Batchelor and Bowden (1985), Frost et al. (2001) and Pearce et al. (1984).

Analytical quality and data interpretation considerations. The geochemical results were interpreted within the limitations of the analytical dataset. Major-element compositions were used primarily to evaluate magmatic differentiation and classification, while trace-element and rare-earth-element distributions were assessed as indicators of magmatic evolution and rare-metal fertility. Analytical detection limits and non-detect values were retained as reported by the laboratory rather than assigned arbitrary concentrations. Where detailed mineralogical data were unavailable, interpretations of REE hosting phases and definitive LCT–NYF classification were treated cautiously. Laboratory analytical certificates, instrument specifications, calibration procedures, reference materials, precision, accuracy, and detection limits should accompany the final submission where required by the target journal.

4. 0 Geology

4.1 Field Geology

Mapping identified migmatitic gneiss, leucogranite and pegmatite as the principal lithological units. The migmatitic gneiss is medium- to coarse-grained, strongly foliated and dominated by quartz, feldspar and biotite. Leucogranite is coarse-grained and leucocratic, consisting mainly of quartz, K-feldspar, plagioclase and biotite.

Pegmatites are the youngest intrusive unit and were mapped at eighteen localities. They occur as discordant veins, ridge-forming bodies and lenticular intrusions in both gneiss and leucogranite. Thickness ranges from approximately 0.6–3.0 m and exposed strike lengths locally exceed 200 m. Fresh exposures show coarse pegmatitic textures, whereas weathered surfaces display feldspar kaolinization, iron-oxide staining and lateritic development. Quartz-rich cores occur locally.

The field relationships indicate a relative sequence in which the migmatitic gneiss represents the principal country rock, followed by emplacement of leucogranitic bodies and subsequent intrusion of pegmatites. The cross-cutting relationships and discordant geometries of the pegmatites provide field evidence for their younger intrusive nature.

Mapping identified migmatitic gneiss, leucogranite and pegmatite as the principal lithological units **(Fig. 2**).

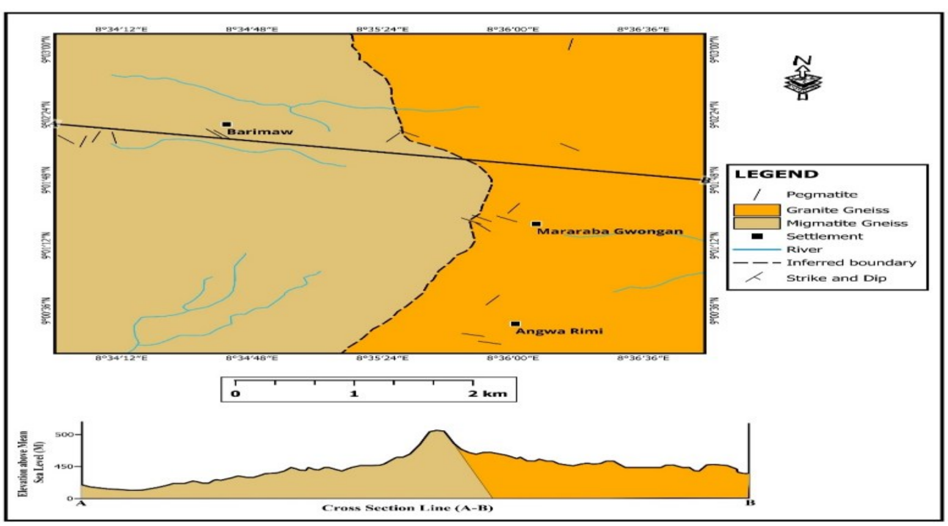

Fig. 2***: Geological Map of the Study Area***

4.2 Structural Characteristics

Structural measurements indicate dominant NE–SW, ENE–WSW and N–S trends with subordinate NW–SE orientations. Most pegmatites dip steeply at 80–90°. A representative vein strikes about 130° and dips 90°, while some ridge-forming bodies strike between 160° and 180°. Minor brittle deformation includes local left-lateral displacement, and quartz veins commonly parallel the dominant pegmatite orientations. The dominant orientations of pegmatite veins and fractures are illustrated by the rose diagrams (Figs. 3 and 4), which demonstrate their close correspondence . The close correspondence between the dominant orientations of pegmatite veins and fracture systems (Figs. 3 and 4) suggests that pre-existing structural discontinuities influenced the emplacement pathways of the pegmatitic melts

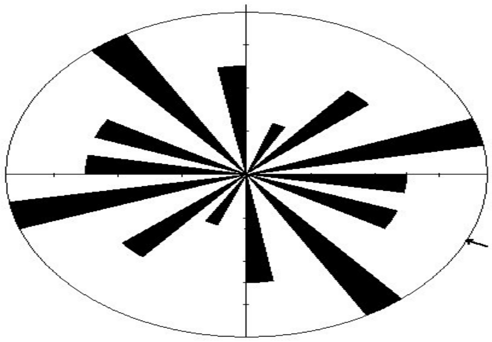

Fig. 3: Ross Diagram of the Veins within the study the Study Area

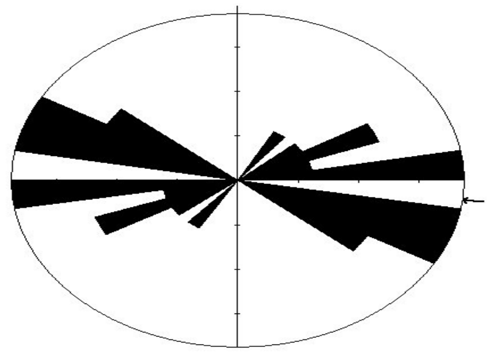

Fig. 4: Ross Diagram for Fractures within

The close correspondence between the dominant orientations of pegmatite veins and fracture systems suggests that pre-existing structural discontinuities influenced the emplacement pathways of the pegmatitic melts. The steep dips and repeated occurrence of pegmatites along these orientations further indicate that the structural framework exerted an important control on their distribution.

4.3 Major-Element Geochemistry

Major oxide compositions are presented in Table 1. SiO_2 ranges from 53.5–92.5 wt.%, Al_2O_3 from 3.2–22.2 wt.% and Fe_2O_3 from 0.39–16.0 wt.%. CaO ranges from 0.27–20.20 wt.% and TiO_2 is generally low. Na_2O ranges from below detection to 3.99 wt.%, K_2O from 0.93–19.40 wt.%, while MgO is absent or very low in most samples. MnO ranges from 0.008–1.32 wt.% and P_2O_5 from 1.64–3.44 wt.%. Although most samples display felsic to highly evolved compositions, several samples show comparatively elevated Fe_2O_3, CaO, Al_2O_3 or K_2O contents. These compositional deviations may reflect mineralogical heterogeneity, localized alteration, incorporation of host-rock material or differences in the proportions of major mineral phases. Consequently, individual anomalous compositions are interpreted cautiously when evaluating whole-rock magmatic trends.

Harker variation diagrams show decreasing MgO, Fe_2O_3, TiO_2, CaO and P_2O_5 with increasing SiO_2, while Al_2O_3 also generally decreases with moderate scatter. Na_2O and K_2O show greater dispersion.

4.5 Alumina Saturation Characteristics

A/CNK values range from approximately 0.59–1.45. Most samples fall within the metaluminous field, with several extending into weakly peraluminous compositions; none plots in the strongly peralkaline field.

4.4 Major-Element Variation Trends

The A/CNK–A/NK relationships indicate predominantly metaluminous compositions, with some samples extending into the peraluminous field. The observed range suggests variable alumina saturation among the analyzed samples rather than a uniformly peraluminous system.

4.6 Trace-Element Geochemistry

Trace-element concentrations are presented in Table 2. Rb concentrations range from approximately 73–4900 ppm, whereas Sr ranges from 14.9–1710 ppm. Cs reaches approximately 128 ppm, Nb ranges from below detection to 224 ppm, and Ta reaches 49.4 ppm. Sn concentrations range from approximately 3.9–1090 ppm, while Ba, Zr, Y and Pb reach maximum concentrations of 2580, 471, 94.7 and 96.6 ppm, respectively. Sn varies from approximately 3.9–1090 ppm, Ba from 80–2580 ppm, Zr from 22–471 ppm, Y from 6.1–94.7 ppm and Pb from 12.8–96.6 ppm.

4.7 K/Rb Variation

The K/Rb versus Rb diagram shows a general decrease in K/Rb ratios as Rb increases. Samples GG001 and GG004 have relatively low K/Rb and elevated Rb, whereas GG007, GG008, GG012 and GG018 show comparatively higher K/Rb and lower Rb. The remaining samples define an intermediate trend.

The progressive decrease in K/Rb with increasing Rb indicates increasing enrichment of Rb relative to K, consistent with progressive magmatic differentiation and preferential incorporation of K into early-forming K-bearing minerals.

Table 1: Major Oxides

Table 1a: Major Oxide Concentrations (Wt %) — GG 001 to GG 011

Major Oxide (Wt %)	GG 001	GG 002	GG 004	GG 005	GG 006	GG 007	GG 008	GG 009	GG 010	GG 011
SiO_2	62.4	62.5	53.5	69.1	69.9	92.5	82.9	68.8	64.7	68.6
TiO_2	ND	0.561	0.142	0.0271	ND	0.0355	0.0978	0.0427	0.0313	ND
Na_2O	1.96	1.13	ND	3.54	3.31	ND	ND	2.64	1.35	3.42
MgO	ND	ND	ND	ND	ND	ND	ND	ND	ND	ND
Al_2O_3	14.1	15.3	22.2	14.1	13.5	3.2	8.26	14.5	15.5	14.4
MnO	0.0834	0.535	0.0383	0.802	1.32	0.0267	0.0081	0.335	0.29	0.0531
P_2O_5	2.11	2.18	2.16	3.06	2.59	1.76	1.64	3.44	2.7	2.92
K_2O	17.6	1.22	19.4	4.94	6.4	1.67	5.14	6.71	8.88	7.22
CaO	0.587	0.284	0.386	1.48	0.841	0.273	0.46	0.859	3.51	2.42
Fe_2O_3	0.498	16	1.48	2.45	1.85	0.393	1.26	2.18	2.43	0.698
$Na_2O + K_2O$	19.56	2.35	NA	8.48	9.71	NA	NA	9.35	10.23	10.64
A/CNK (A SI)	0.60	4.14	1.02	1.02	0.97	1.39	1.29	1.10	0.85	0.81

Table 1b: Major Oxide Concentrations (Wt %) — GG 012 to GG 003

Major Oxide (Wt %)	GG 012	GG 013	GG 014	GG 015	GG 016	GG 017	GG 018	GG 003
SiO_2	74.5	73.6	72.7	56.3	71.4	67.0	70.8	60.8
TiO_2	ND	ND	ND	0.53	ND	ND	0.13	1.2
Na_2O	1.77	3.8	3.99	1.03	3.84	3.07	1.65	1.53
MgO	ND	ND	ND	0.306	ND	ND	ND	0.659
Al_2O_3	11.1	13.5	13.9	11.2	15.3	14.4	11.1	11.3

MnO	0.0301	0.0273	0.146	0.21	0.213	0.58	0.0585	0.171
P_2O_5	1.97	2.71	3.09	2.00	3.35	3.34	1.87	2.07
K_2O	2.16	4.22	3.11	0.932	2.54	7.61	3.10	7.86
CaO	7.38	0.888	1.63	20.2	0.805	1.36	8.23	5.57
Fe_2O_3	0.627	0.927	1.04	6.85	2.18	2.18	2.60	8.01
$Na_2O + K_2O$	3.93	8.02	7.10	1.96	6.38	10.68	4.75	9.39
A/CNK (A SI)	0.59	1.09	1.08	0.28	1.45	0.91	0.53	0.53

Note: ND = not detected; NA = not available.

Table 2: Trace Element Concentration within the Pegmatite Sample
Table 2a: Trace Element Concentrations (ppm) — GG 001 to GG 011

Trace Element (ppm)	GG 001	GG 002	GG 004	GG 005	GG 006	GG 007	GG 008	GG 009	GG 010	GG 011
Cr	ND	137	ND	ND	ND	ND	ND	ND	ND	ND
Cu	97.8	94.1	38.2	81	101	157	128	54.7	57.2	107
Ni	13.9	59.3	18.6	25.6	24.8	51	43.8	ND	ND	33.6
Zn	225	261	30.5	157	82.2	77.9	68.1	245	139	76.2
Rb	3860	184	4900	928	1040	73.2	203	2170	1780	769
Sr	93.6	142	133	139	152	14.9	16.1	173	865	128
Y	15.6	20.8	27.2	9.06	18.4	7.53	9.27	9.65	15.7	7.39
Zr	21.9	400	95.4	41.6	184	22.3	57.4	124	167	57.4
Mo	ND	ND	ND	ND	ND	ND	ND	ND	ND	ND
Sn	6.63	24.2	10.1	191	40.2	7.34	7.4	213	281	58.8
Ba	236	475	170	185	294	98.7	232	80	1300	150
Sc	ND	ND	ND	ND	ND	ND	ND	ND	ND	ND
Nb	ND	70.9	ND	29	9.4	6.88	11.4	86.9	224	119
Cs	128	ND	85.1	12.5	ND	ND	ND	45.4	48.7	48.9
Ta	ND	ND	ND	ND	ND	ND	ND	ND	ND	ND
Hf	ND	ND	ND	ND	ND	ND	ND	ND	ND	ND
Pb	72.2	71.7	49.6	29.7	42	20.2	26.2	12.8	19	31.3
V	ND	232	ND	ND	ND	ND	77.1	ND	ND	ND

Table 2b: Trace Element Concentrations (ppm) — GG 012 to GG 003

Trace Element (ppm)	GG 012	GG 013	GG 014	GG 015	GG 016	GG 017	GG 018	GG 003
Cr	ND	ND	64	ND	ND	ND	ND	ND
Cu	147	83.8	76.7	105	167	75.6	103	182
Ni	44.4	19.8	19.7	61.1	50	ND	42	59.7
Zn	51.4	57.5	67.4	150	107	174	54.3	224
Rb	101	852	601	154	477	1980	172	855
Sr	1710	115	144	389	156	400	1670	1060
Y	18.9	6.1	15.5	94.7	9.97	13.9	24.7	46.4
Zr	233	39.6	68.3	215	201	79.4	257	471

Mo	ND	ND	ND	ND	ND	ND	ND	ND
Sn	ND	674	1090	883	357	158	9.03	3.87
Ba	652	109	99.4	299	132	349	1180	2580
Sc	ND	ND	769	ND	ND	ND	ND	ND
Nb	ND	46.4	119	27.5	62.8	160	4.58	20.6
Cs	ND	22.4	ND	ND	19.2	71.4	ND	91.9
Ta	ND	13.7	49.4	ND	ND	ND	ND	ND
Hf	ND	ND	ND	ND	ND	ND	ND	ND
Pb	30.2	24.3	16.6	27.1	29.5	64	30.2	96.6
V	ND	ND	ND	ND	ND	ND	ND	164

Note: ND = not detected.

Table 3: Concentration of REE within the Pegmatite of the Study Area

Table 3a: Rare Earth Element Concentrations — La to Sc

Sample ID	La	Ce	Pr	Nd	Sc
Gw001	47	ND	ND	100	ND
Gw002	ND	176	ND	26.9	ND
Gw003	73.3	ND	ND	ND	ND
Gw004	ND	ND	ND	ND	75
Gw005	ND	320	ND	ND	ND
Gw006	86.3	ND	ND	64	ND
Gw007	ND	ND	ND	ND	ND
Gw008	ND	ND	ND	ND	ND
Gw009	ND	78.6	ND	29.3	ND
Gw010	ND	ND	ND	ND	ND
Gw011	99.9	157	68.3	67.5	ND
Gw012	96.54	ND	ND	ND	ND
Gw013	160	ND	ND	32	ND
Gw014	ND	35	ND	78	ND
Gw015	ND	ND	ND	31	ND
Gw016	ND	ND	17	ND	ND
Gw017	ND	91	ND	ND	ND
Gw018	137	242	189	19.4	234

Table 3b: Rare Earth Element Concentrations — Dy to Ho

Sample ID	Dy	Y	Yb	Lu	Eu	Ho
Gw001	74	15.6	ND	ND	ND	ND
Gw002	ND	28	ND	ND	ND	ND
Gw003	15	27.2	ND	ND	ND	ND
Gw004	ND	9.6	ND	ND	ND	ND
Gw005	ND	18.4	ND	ND	ND	ND
Gw006	90	27.53	ND	ND	ND	ND
Gw007	146	9.27	ND	ND	ND	ND
Gw008	ND	9.65	ND	ND	ND	ND

Gw009	ND	15.7	ND	ND	ND	ND
Gw010	ND	7.39	ND	ND	ND	ND
Gw011	58	18.9	ND	ND	ND	ND
Gw012	ND	6.1	ND	ND	ND	ND
Gw013	177	15.5	ND	ND	ND	ND
Gw014	ND	94.7	ND	ND	ND	ND
Gw015	ND	9.97	ND	ND	ND	ND
Gw016	ND	13.9	ND	ND	ND	ND
Gw017	223	24.7	ND	ND	ND	ND
Gw018	ND	46.4	ND	ND	ND	ND

Note: ND = not detected. *Lu* should be written as Lu, not “lu”, in the final manuscript.

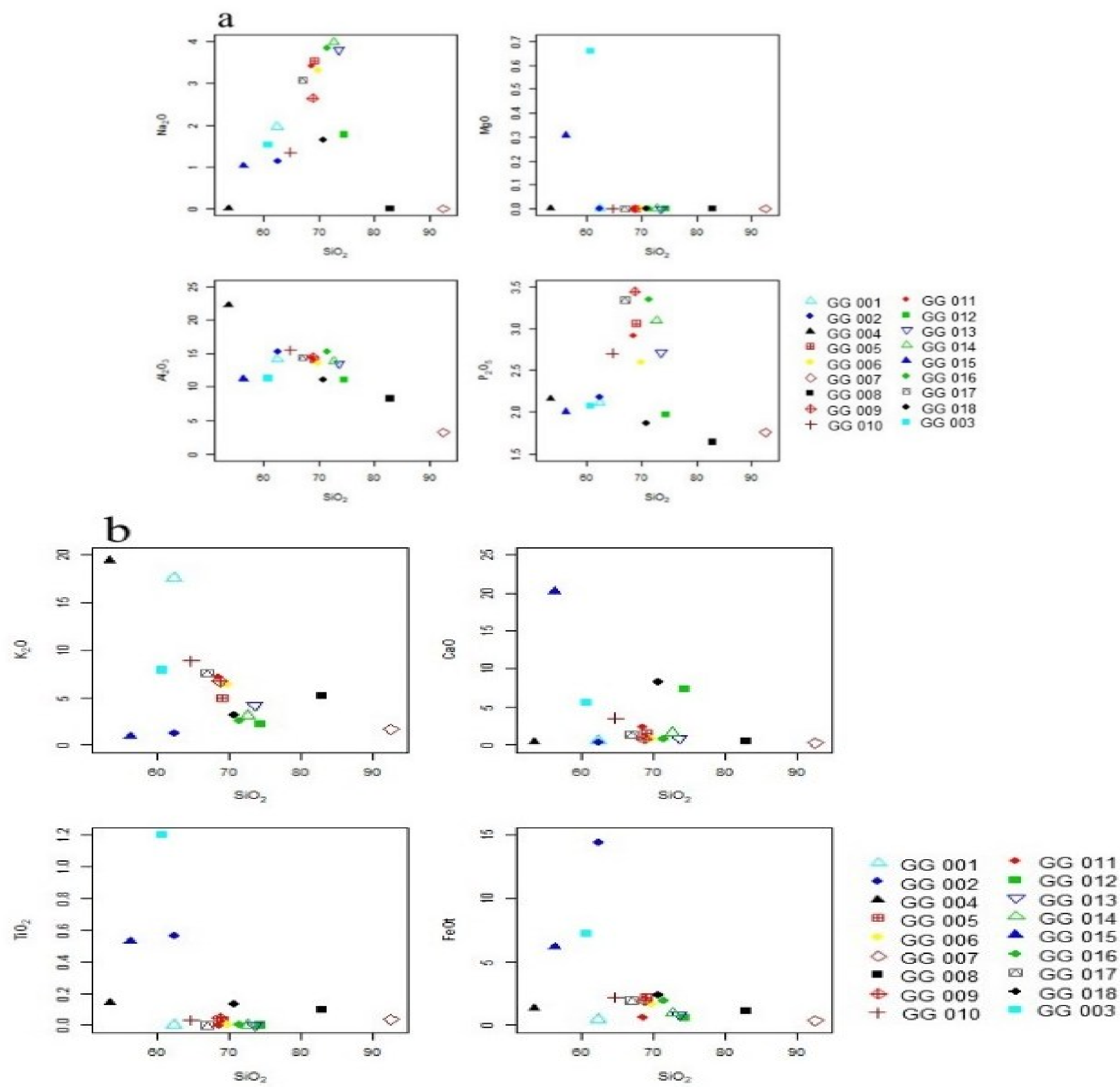

Fig. 5: Harker Variation Diagram

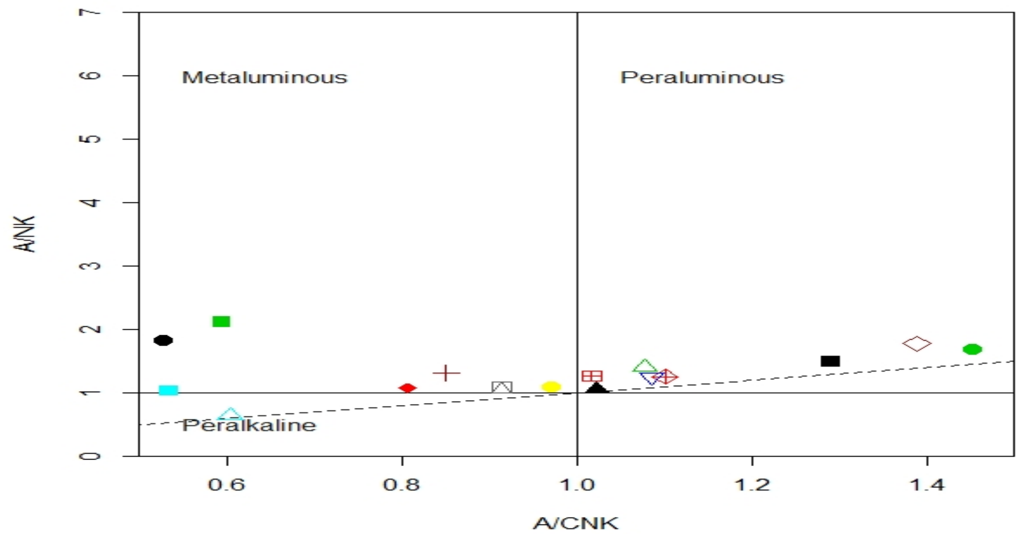

Fig. 6: Aluminum Saturation Index

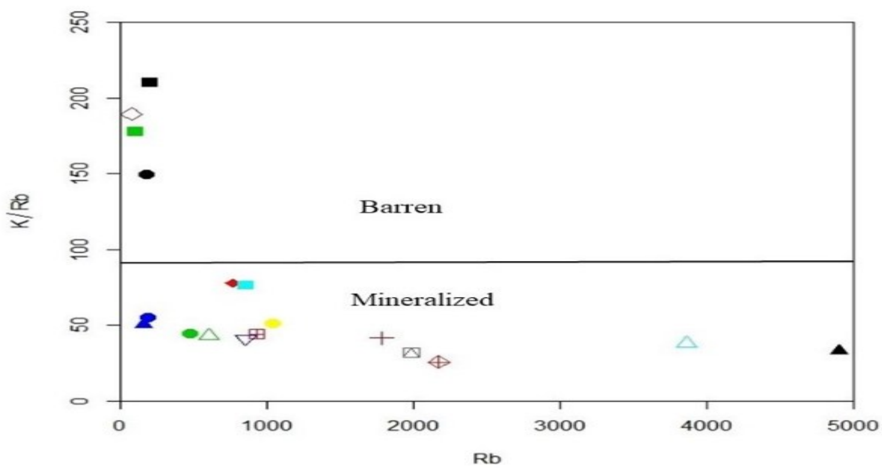

Fig. 7: Variation diagram of K/Rb vs Rb

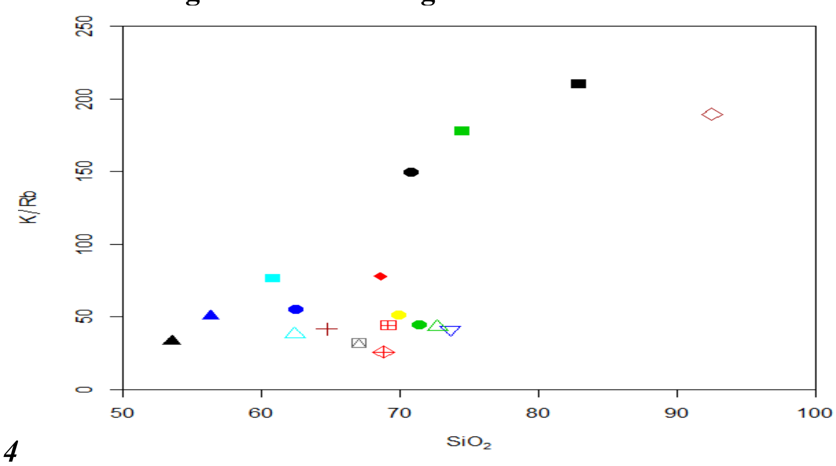

4

Fig. 8: plot of K/Rb vs Sio₂

4.8 K/Rb versus SiO_2 Variation

The K/Rb versus SiO_2 diagram shows an inverse relationship. Samples with approximately 55–65 wt.% SiO_2 generally have higher K/Rb ratios, whereas samples above 70 wt.% SiO_2 display progressively lower K/Rb values. The K/Rb–SiO_2 relationship shows an overall inverse trend, with higher-SiO_2 samples generally characterized by lower K/Rb ratios. This pattern is consistent with progressive enrichment of Rb during magmatic evolution, although the scatter indicates that the differentiation process was not uniform across all samples.

4.9 K/Rb versus Cs Variation

The K/Rb versus Cs diagram shows a broad inverse relationship: most samples have low to intermediate Cs and moderate K/Rb, whereas relatively Cs-rich samples tend to have lower **K/Rb ratios.**

The SiO_2–K_2O relationships show substantial compositional variation among the analyzed samples, extending from relatively low-K compositions to strongly K-enriched compositions. Because the samples represent highly evolved pegmatitic and related felsic rocks, the classification fields are used primarily as comparative indicators of compositional affinity rather than as definitive evidence of a specific volcanic series**.**

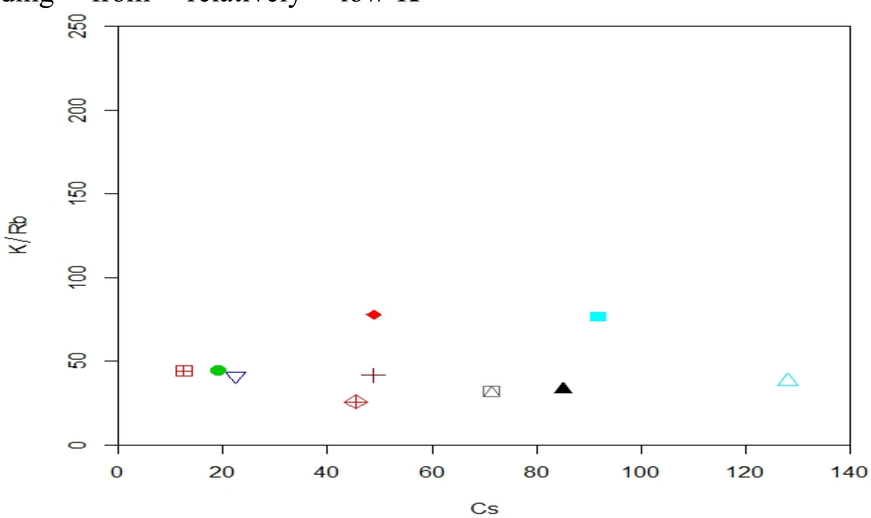

Fig. 9: Plot of K/Rb Vs Cs

4.10 SiO_2–K_2O Relationships

“The SiO_2–K_2O diagram (**Fig. 10**) places the analyzed samples across tholeiitic, calc-alkaline, high-K calc-alkaline and shoshonitic fields, with most samples occurring in the calc-alkaline to high-K calc-alkaline fields

.

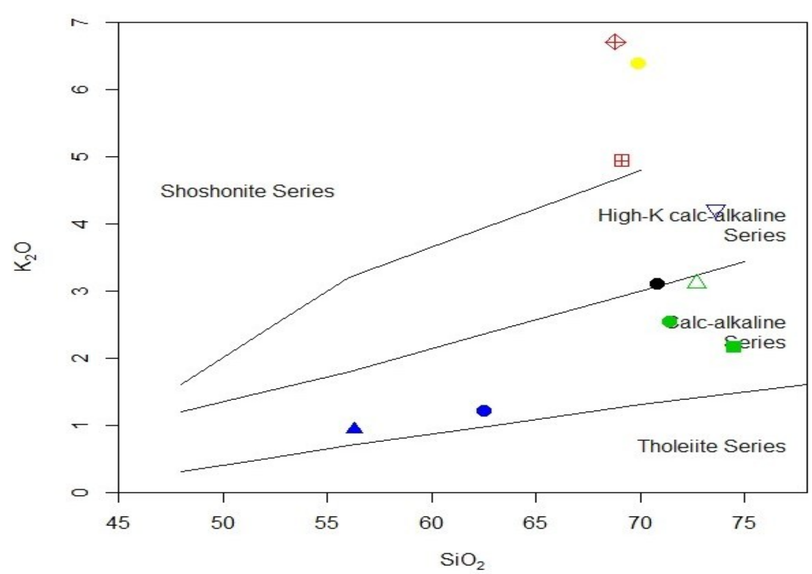

Fig. 10:SiO_2–K_2O Relationships

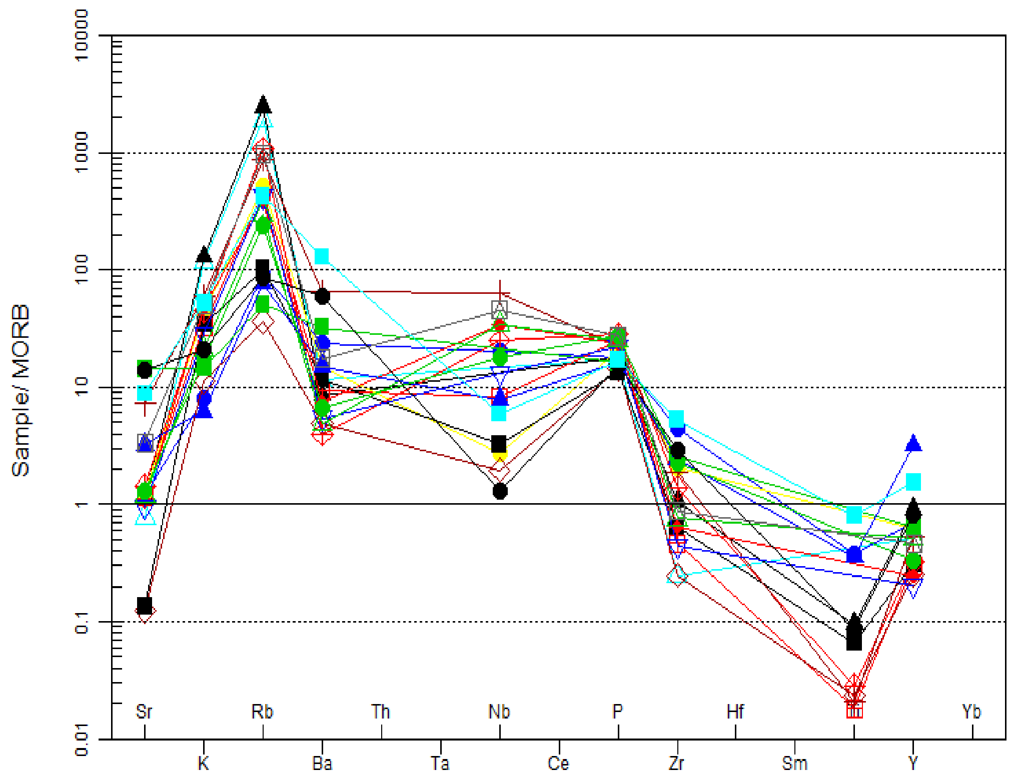

Fig. 11: MORB spider Diagram

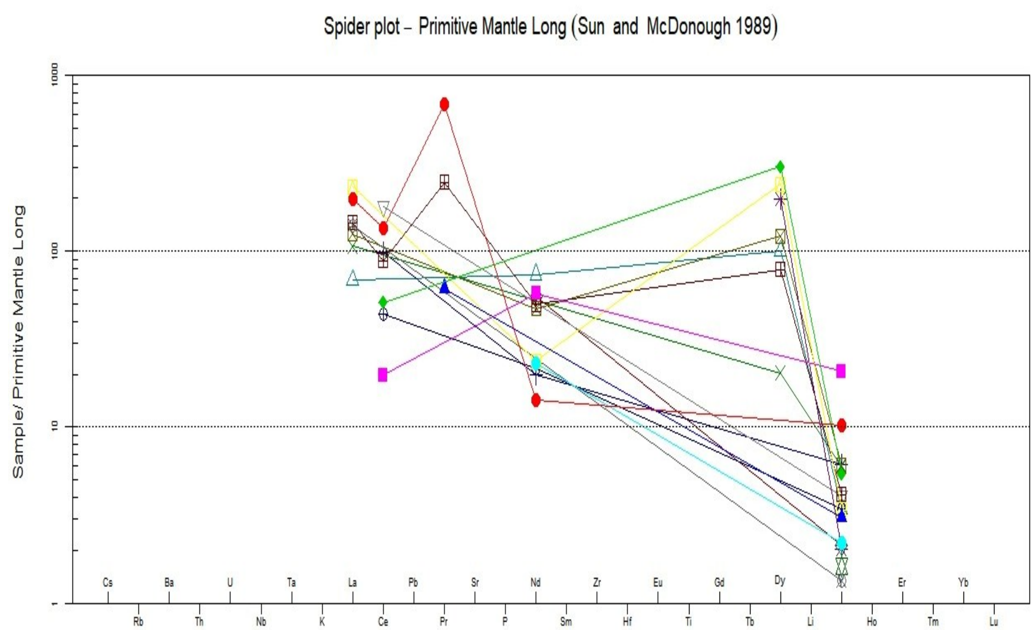

Fig. 12: Spider Plot-Primitive Mantle (Sun and McDonough 1989)

4.12 Tectonomagmatic Classification

The R_1–R_2 discrimination diagram places most samples in the late- to post-orogenic granitoid field, with fewer samples in the anorogenic field and some near the syn-collisional/late- to post-orogenic boundary.

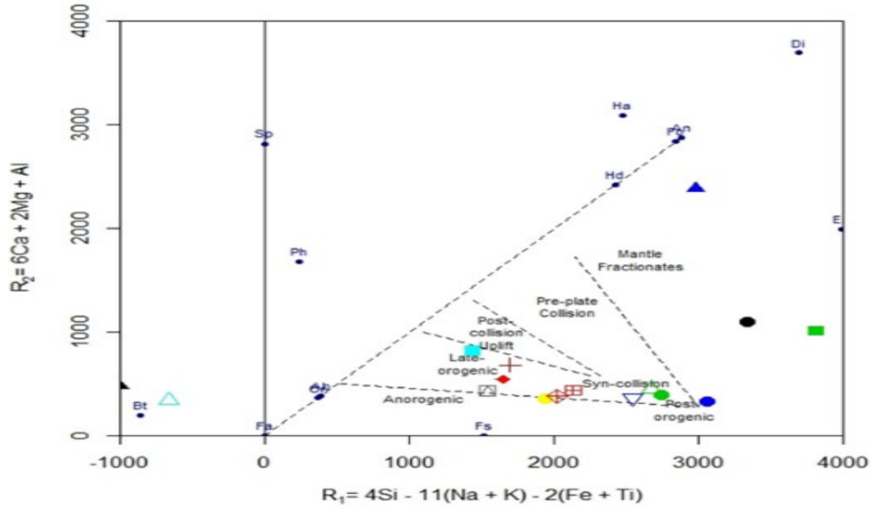

Fig. 13: R_1–R_2 Tectonomagmatic Discrimination Diagram for the Gwon-Gwon Pegmatites

5.0 Discussion

5.1 Petrogenesis and Magmatic Evolution

The integrated field, structural and geochemical evidence indicates that the Gwon-Gwon pegmatites represent highly evolved felsic melts emplaced during the late stages of Pan-African granitic magmatism. Field relationships show that the pegmatites cross-cut migmatitic gneisses and leucogranites, confirming their younger intrusive relationship with the surrounding basement rocks. Their occurrence as discordant veins, ridge-forming bodies and lenticular intrusions, together with their close association with fractures and shear zones, suggests that the emplacement of the pegmatitic melts was strongly influenced by pre-existing crustal discontinuities.

The major-element data provide evidence for progressive magmatic differentiation. The general decrease in MgO, Fe_2O_3, TiO_2, CaO and P_2O_5 with increasing SiO_2 (Fig. 5) is consistent with the progressive removal of mafic and accessory minerals during crystallization. The observed trends can be attributed to the fractionation of ferromagnesian minerals, feldspars, Fe–Ti oxides and apatite from the evolving melt. The wide range of SiO_2 contents (53.5–92.5 wt.%) further indicates substantial chemical variation within the sampled pegmatitic system. The relatively high SiO_2 contents of several samples, coupled with generally low MgO and TiO_2, are characteristic of highly evolved felsic compositions.

The A/CNK values of 0.59–1.45 indicate that the samples range from metaluminous to weakly peraluminous compositions (Fig. 6). The predominance of metaluminous compositions suggests that the Gwon-Gwon pegmatites did not evolve exclusively from strongly peraluminous melts. Instead, the observed compositional range may reflect variable degrees of fractionation, mineral accumulation and/or interaction between evolved melts and their host rocks. Consequently, the geochemical characteristics are more consistent with an evolved granitic-pegmatitic system than with a single compositionally uniform magma.

5.2 Fractional Crystallization and Rare-Metal Enrichment

The trace-element distributions provide additional evidence for progressive fractional crystallization. Rb concentrations range from 73 to 4,900 ppm, whereas Sr varies from 14.9 to 1,710 ppm. The generally inverse relationship between K/Rb and Rb (Fig. 7) is particularly significant because Rb preferentially enters the residual melt as K-bearing minerals crystallize. Thus, decreasing K/Rb ratios accompanied by increasing Rb concentrations indicate progressive enrichment of incompatible elements during magmatic evolution.

The relationship between K/Rb and SiO_2 (Fig. 8) provides complementary evidence for differentiation. Samples with relatively low SiO_2 generally display higher K/Rb ratios, whereas more silica-rich samples tend to have lower K/Rb values. This pattern suggests that increasing silica enrichment was accompanied by progressive removal of K-bearing minerals and concentration of Rb in the residual melt. Similarly, the inverse K/Rb–Cs relationship (Fig. 9) indicates that Cs became progressively concentrated in the more evolved portions of the system.

The enrichment of Rb, Cs, Sn, Nb and Ta in several samples is particularly relevant to the rare-metal character of the pegmatites. Sn concentrations reach approximately 1,090 ppm, Nb reaches about 224 ppm and Ta reaches 49.4 ppm, while Cs reaches approximately 128 ppm. These elements are generally incompatible during the early stages of granitic crystallization and therefore become concentrated in residual melts during advanced differentiation. The coexistence of these elements indicates that the Gwon-Gwon pegmatites experienced substantial magmatic evolution and developed appreciable rare-metal fertility. However, the heterogeneous concentrations among samples suggest that differentiation was spatially variable within the pegmatite field rather than uniform throughout the entire system.

5.3 Rare-Earth Element Characteristics and Pegmatite Classification

The REE and multi-element data further demonstrate considerable chemical differentiation within the Gwon-Gwon pegmatites. The primitive-mantle-normalized multi-element patterns (Fig.s 11 and 12) show variable enrichment in incompatible elements, including Nb, Ta, Sn, Y and REEs. The REE data also show substantial sample-to-sample variability, with some samples displaying relatively elevated La, Ce, Nd, Dy and Y concentrations, whereas several REEs are below detection limits in other samples. This heterogeneity may reflect differences in mineral assemblage, degree of fractionation and the distribution of REE-bearing accessory minerals within individual pegmatite bodies.

Where observable, the REE patterns generally indicate greater enrichment of LREE relative to HREE, accompanied by variable Eu behaviour. Such variability may be related to feldspar crystallization, because Eu can be preferentially incorporated into feldspar, particularly under conditions where Eu^{2+} is stable. Consequently, Eu anomalies may provide evidence for feldspar-controlled differentiation of the parental granitic melt. However, because the present dataset is based principally on whole-rock chemistry and does not identify the specific REE-bearing minerals, the observed REE patterns should be interpreted as evidence of geochemical fertility rather than direct evidence of economic REE mineralization.

The combined enrichment in Rb, Cs, Sn, Nb, Ta and REEs demonstrates an evolved rare-metal signature. Nevertheless, classification of the pegmatites exclusively as LCT or NYF is not fully justified by the available dataset. LCT pegmatites are typically characterized by Li–Cs–Ta enrichment and strong peraluminous affinities, whereas NYF pegmatites are commonly associated with Nb–Y–F enrichment and metaluminous to weakly peraluminous parental granites. The Gwon-Gwon samples exhibit characteristics of both groups, including significant Rb–Cs–Sn enrichment together with Nb–Ta–Y and REE enrichment. The variable A/CNK values also do not support a uniformly strongly peraluminous system. Therefore, the available evidence is more appropriately interpreted as indicating a transitional or mixed LCT–NYF geochemical affinity, rather than assigning the entire field unequivocally to either family.

Definitive classification would require mineralogical evidence, particularly identification of Li-bearing minerals, Nb–Ta oxides, REE-bearing phases and other diagnostic accessory minerals. Electron-microprobe analysis, SEM–EDS, LA-ICP-MS mineral chemistry and isotopic studies would provide useful constraints on mineral hosts, melt sources, fractionation processes and the LCT–NYF classification of the pegmatites.

5.4 Tectonic and Structural Implications

The tectonomagmatic characteristics of the Gwon-Gwon pegmatites are consistent with emplacement during the late to post-orogenic stages of Pan-African granitic magmatism. The R_1–R_2 discrimination diagram (Fig. 13) places most samples within the late- to post-orogenic field, with fewer samples plotting in the anorogenic field and some occurring close to the boundary between syn-collisional and late- to post-orogenic fields. These relationships suggest that the pegmatites were generated and emplaced during the waning stages of regional tectonothermal activity rather than during the earliest stages of continental collision.

The structural data provide further support for this interpretation. Pegmatites predominantly follow NE–SW, ENE–WSW and N–S orientations, with subordinate NW–SE trends, and most bodies are steeply dipping at approximately 80–90°. The close correspondence between pegmatite and fracture orientations shown by the rose diagrams indicates that pre-existing fractures and shear zones provided important pathways for the migration and emplacement of evolved melts. The occurrence of quartz veins along similar structural orientations further suggests that these discontinuities remained permeable during late-stage hydrothermal activity.

The structural framework therefore appears to have exerted a dual control on the evolution of the pegmatite system: it provided pathways for the migration of residual melts and subsequently facilitated the movement of late-stage fluids. Intersections between fractures and local brittle reactivation may have enhanced permeability and created favourable sites for pegmatite thickening and mineral concentration. The observed relationship between structural architecture and geochemical enrichment suggests that exploration for rare-metal mineralization should consider both geochemical anomalies and structurally favourable zones, particularly fracture intersections and shear-related pegmatite bodies.

5.5 Integrated Model of Pegmatite Evolution

The combined geological, structural and geochemical evidence supports a model in which the Gwon-Gwon pegmatites developed from evolved residual melts generated during Pan-African granitic magmatism. Progressive crystallization of the parental granitic magma resulted in the removal of major rock-forming and accessory minerals and consequent enrichment of incompatible elements such as Rb, Cs, Nb, Ta, Sn and REEs in the residual melt. During the late stages of magmatic evolution, these volatile- and incompatible-element-rich melts migrated through pre-existing fractures, shear zones and other crustal discontinuities.

The resulting pegmatites were subsequently emplaced as discordant veins, lenses and ridfThe rosege-forming bodies within migmatitic gneisses and leucogranites. Continued fractionation produced marked geochemical variability among individual pegmatite bodies, reflected by the wide ranges of Rb, Sr, Cs, Nb, Ta, Sn, Y and REE concentrations. The structural control on emplacement, combined with the observed incompatible-element enrichment, indicates that the Gwon-Gwon pegmatite field represents a chemically evolved and structurally controlled rare-metal system.

Overall, the evidence supports a late- to post-orogenic, structurally controlled, highly differentiated pegmatitic system with mixed/transitional LCT–NYF characteristics. Although the geochemical results demonstrate significant rare-metal fertility, further mineralogical and mineral-chemical investigations are required to establish the identity, distribution and economic significance of the REE- and rare-metal-bearing phases.

5.6 Limitations and Implications for Further Work

The present interpretation is based principally on field relationships, structural observations, whole-rock major-element chemistry, and trace-element/REE distributions. Although these data provide strong evidence for advanced magmatic differentiation and rare-metal fertility, they do not by themselves establish the mineral hosts of the REEs or demonstrate an economic mineral resource. Detailed petrography, scanning electron microscopy with energy-dispersive spectroscopy, electron-microprobe analysis, and, where appropriate, LA-ICP-MS mineral chemistry would help identify REE-bearing phases and further resolve the LCT–NYF affinity and source characteristics of the pegmatites. Additional channel or trench sampling and systematic mineralogical studies would also improve the basis for evaluating the continuity and economic significance of the identified geochemical anomalies.

6.0 Conclusion

The Gwon-Gwon area is underlain mainly by migmatitic gneiss, leucogranite and pegmatite. Eighteen pegmatite occurrences were mapped as discordant, ridge-forming and lenticular bodies, commonly following NE–SW, ENE–WSW, N–S and subordinate NW–SE structures. Geochemical data indicate progressive fractional crystallization, as expressed by decreasing compatible major oxides, declining K/Rb ratios, and enrichment in Rb, Cs, Nb, Ta, Sn, and REEs. The pegmatites are predominantly metaluminous to weakly peraluminous and are most consistent with evolved granitic magmatism in a late- to post-orogenic Pan-African setting. Their structural position and incompatible-element enrichment indicate significant rare-metal fertility. Further mineralogical and targeted geochemical work is recommended to determine the distribution and economic significance of REE and associated critical-metal mineralization.

7.0 References

Abaa, S. I. (1983). Petrology and geochemistry of Pan-African granitoids in north-central Nigeria. *Journal of African Earth Sciences, 1*(1), 57–65.

Batchelor, R. A., & Bowden, P. (1985). Petrogenetic interpretation of granitoid rock series using multicationic parameters. *Chemical Geology, 48*, 43–55.

Černý, P. (1991). Rare-element granitic pegmatites. Part I: Anatomy and internal evolution of pegmatite deposits. *Geoscience Canada, 18*(2), 49–67.

Černý, P., & Ercit, T. S. (2005). The classification of granitic pegmatites revisited. *The Canadian Mineralogist, 43*, 2005–2026.

Chappell, B. W., & White, A. J. R. (1974). Two contrasting granite types. *Pacific Geology, 8*, 173–174.

Dada, S. S. (2006). Proterozoic evolution of Nigeria. In O. O. Oshin (Ed.), *The Basement Complex of Nigeria and Its Mineral Resources* (pp. 29–44).

Ekwueme, B. N., & Matheis, G. (1995). Rare-metal pegmatites of southeastern Nigeria. *Journal of African Earth Sciences, 20*(4), 389–397.

El-Bouseily, A. M., & El-Sokkary, A. A. (1975). The relation between Rb, Ba and Sr in granitic rocks. *Chemical Geology, 16*, 207–219.

Frost, B. R., Barnes, C. G., Collins, W. J., Arculus, R. J., Ellis, D. J., & Frost, C. D. (2001). A geochemical classification for granitic rocks. *Journal of Petrology, 42*(11), 2033–2048.

Irvine, T. N., & Baragar, W. R. A. (1971). A guide to the chemical classification of the common volcanic rocks. *Canadian Journal of Earth Sciences, 8*, 523–548.

Obaje, N. G. (2009). *Geology and Mineral Resources of Nigeria*. Springer.

Oyawoye, M. O. (1972). The Basement Complex of Nigeria. In *African Geology*.

Pearce, J. A., Harris, N. B. W., & Tindle, A. G. (1984). Trace element discrimination diagrams for the tectonic interpretation of granitic rocks. *Journal of Petrology, 25*(4), 956–983.

Rahaman, M. A. (1988). Recent advances in the study of the Basement Complex of Nigeria. In *Precambrian Geology of Nigeria* (pp. 11–43).

Shand, S. J. (1943). *Eruptive Rocks: Their Genesis, Composition, Classification and Their Relation to Ore Deposits* (2nd ed.). Thomas Murby & Co.

Sun, S. S., & McDonough, W. F. (1989). Chemical and isotopic systematics of oceanic basalts: Implications for mantle composition and processes. In A. D. Saunders & M. J. Norry (Eds.), *Magmatism in the Ocean Basins* (pp. 313–345). Geological Society Special Publication No. 42.

Declarations

Funding

The authors received no financial support for the research, authorship, and/or publication of this article.

Ethical Approval

Not applicable

Informed Consent

Not applicable.

Consent for Publication

Not applicable.

Declaration of Competing Interests

The authors declared no competing interests

Data Availability Statement

Data shall be made available upon request

Conflict of Interest

The authors declared no conflict of interest

Authors' Contributions

Manalaku Yele Pes contributed to the conceptualization, field geological mapping, sample collection, structural data acquisition, geochemical data analysis, interpretation of results, and preparation of the manuscript. N. G. Goki contributed to the study design, supervision of fieldwork, interpretation of geological and geochemical data, and critical review of the manuscript. Benson S. Jatau contributed to geochemical interpretation, data validation, literature review, manuscript review, and editing. All authors read and approved the final manuscript.